2013 IEEE 10th International Symposium on Biomedical Imaging:
From Nano to Macro
San Francisco, CA, USA, April 7-11, 2013

A HYBRID MULTI-SCALE APPROACH TO AUTOMATIC AIRWAY TREE SEGMENTATION FROM CT SCANS

Ziyue Xu ⋆ *Ulas Bagci* *Brent Foster* *Daniel J. Mollura*

Center for Infectious Disease Imaging (CIDI)
Radiology and Imaging Science Department
National Institutes of Health (NIH), Bethesda, MD 20892

ABSTRACT

Airway structure and morphology is commonly related to inflammatory and infectious lung diseases, and often analyzed non-invasively through high resolution computed tomography (CT) scans. Conventionally, most airway related feature characterization on these scans is performed manually, but is often too labor intensive and time consuming for routine clinical practice. Therefore, semi- and fully-automatic airway segmentation algorithms are crucial for the diagnosis of these conditions. A fundamental challenge in airway tree segmentation is highly variable intensity levels within the lumen, which often causes a segmentation method to leak into adjacent lung parenchyma through blurred airway walls or soft boundaries. In this paper, we present a new hybrid multi-scale airway segmentation approach to solve these problems through proposing a new fuzzy connectivity based algorithm combining multiple features to identify airways at different scales. The performance of the proposed method was qualitatively and quantitatively evaluated on pulmonary CT images from human patients with diverse diseases with promising results.

Index Terms— Airway tree segmentation, fuzzy connectivity, multi-scale vesselness, grayscale morphological reconstruction, region growing

1 Introduction

An accurate analysis of airway tree structure from CT scans provides important information on pulmonary diseases, which usually affect geometry of the airway tree including airway wall thickness. Due to the inherent complexity of airway structure and the resolution limitations of CT, manually tracing and analyzing airways is an extremely tedious task, taking more than seven hours' intensive work per image [1]. Moreover, manual analysis suffers from large variability and poor reproducibility. Therefore, in order to provide quantitative and reliable assessment of lung diseases, semi- and fully-automatic airway segmentation algorithms have become an active area of research over the past decade.

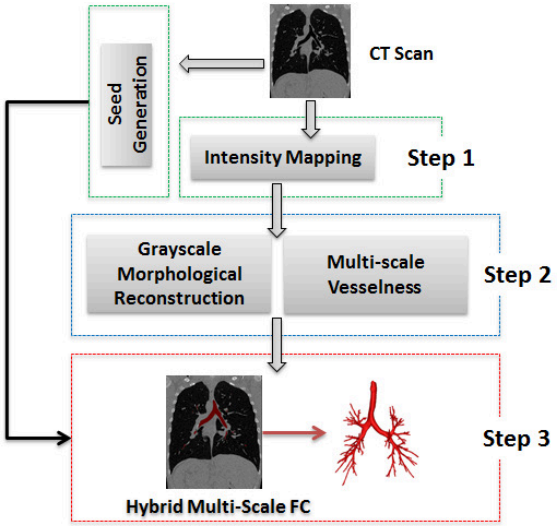

Fig. 1: Flowchart of the airway segmentation algorithm

Many segmentation approaches have been proposed and subsequently investigated in the literature, including rule-based [1], morphology-based [2], classification-based [3], etc. Among these methods, region growing (RG) is probably the mostly used technique for identification of the airways. However, a simple intensity based RG usually leaks into non-object territories (often nearby small airways) owing to partial volume effects, image noise, and artifacts. RG can be considered reliable when analyzing large airway branches, including trachea and principal bronchus, however, incorporating higher level information needs to be considered to identify smaller airways without having any leakage as currently many studies targeting this approach. Alternatively, grayscale morphological reconstruction [2] has been shown to be effective in accurately identifying candidate airways on 2-D CT slices, but is limited to 2-D cross section and does not

⋆ Corresponding author: ziyue.xu@nih.gov. This research is supported by CIDI, the intramural research program of the National Institute of Allergy and Infectious Diseases (NIAID) and the National Institute of Biomedical Imaging and Bioengineering (NIBIB).

U.S. Government work
not protected by U.S. copyright

yield high sensitivity if the airway is not perpendicular to the slice plane. Another approach for better airway identification is based on the enhancement of the vessels (i.e., vesselness filter) [4]. Although this process can further help identify airway locations, it also yields unavoidable false positives over lung area. See [5] for a detailed review on computerized methods for identification and analysis of airways.

In this paper, we developed a novel multi-scale hybrid RG algorithm to segment airway tree in CT images automatically. Our proposed method combines Fuzzy Connectivity (FC) [6] with the RG method to confine the growth process with a predefined *fuzzy affinity* relationship. This relationship is very versatile and convenient for combining several features other than simple intensity features within the framework to improve the final output. Furthermore, multiple strategies were used to restrict the segmentation procedure to only airway regions and achieve a *high sensitivity* with lower leakage accordingly. Fig. 1 illustrates the flowchart representation of the proposed method. As can easily be noted from the flowchart, the proposed method uses intensity based and morphology based methods together; hence it is called hybrid. In step (1), the original CT scan is passed through an intensity mapping filter so that the voxels whose intensity is out of the range [-1000HU, -700HU] get mapped to -1000 or -700 HU. Meanwhile, a seed at trachea is identified automatically by 2-D Hough transform [7]. Then, in step (2), grayscale morphological reconstruction and vesselness are computed and passed together with the seed to FC computation. In step (3), features of local airway structure are incorporated into the theoretical FC model through a new affinity function design. Finally, binary airway tree is produced by thresholding over FC image.

2 Theory and Algorithms

In this section, we first briefly present the basic theory of FC [6], grayscale morphological reconstruction [2], and multi-scale vesselness enhancement [4]. Subsequently, the theory and algorithm of a new region growing approach is formulated that combines the above methods to capture airway branches while avoiding leakage.

2.1 Fuzzy Connectivity

Let $\mathbb{Z}^3$ denote a 3-D cubic grid representing the *image space* where $\mathbb{Z}$ is the set of integers; each element of $\mathbb{Z}^3$ is called a *voxel*. An image on $\mathbb{Z}^3$ may be defined by an *image intensity function* $f : \mathbb{Z}^3 \to \mathbb{Z}$, where $\mathbb{Z}$ is the set of integers. A fuzzy relation $\mu_\alpha : \mathbb{Z}^3 \times \mathbb{Z}^3 \to \{0, 1\}$ referred to as *adjacency* is used to determine closeness of two voxels in the image space. A path π is a sequence $\langle p_1, p_2, ..., p_l\rangle$ where every two successive voxels are adjacent. Path strength $\mu_{\mathcal{N}}(\pi)$ is defined as:

$$\mu_{\mathcal{N}}(\pi) = \min_{1\le i<l} \mu_\kappa(p_i, p_{i+1}) \tag{1}$$

where $\mu_K(p, q)$, referred to as *fuzzy affinity*, captures the local hanging-togetherness between p and q, i.e., the strength of the link $\langle p, q\rangle$. FC between two voxels p, q is the strength of the strongest path, i.e.,

$$\mu_K(p, q) = \max_{\pi\in\mathcal{P}(p,q)} \mu_{\mathcal{N}}(\pi), \tag{2}$$

where, $\mathcal{P}(p, q)$ denotes the set of all paths between p, q. A fuzzy connected object $\mathcal{O}$ in an image is defined as the region grown from a predetermined set of seeds S. Thus, the membership-function of $\mathcal{O}$ can be defined as follows:

$$\mu_{\mathcal{O}}(p) = \max_{s\in S} \mu_K(p, s). \tag{3}$$

An efficient computational solution was presented in [6].

2.2 Grayscale Morphological Reconstruction

In pulmonary CT images, the airway can be regarded as local minima of intensity in a 2-D slice I that can be enhanced by applying grayscale morphological reconstruction. Airway of different diameters are handled using a range of morphological structuring elements (SE) by successive dilation on the basis SE as

$$B_n = B_0 \oplus B_0 \oplus ... \oplus B_0, \tag{4}$$

where B_0 is the smallest 4-connected binary SE and B_n is the n times dilation result of B_0 and $\oplus$ is the dilation operator.
A "marker image" [2] is then constructed from the original image slice I and SE B_n by a grayscale closing $\bullet$ as

$$J_1^n = I \bullet B_n \triangleq (I \oplus B_n) \ominus B_n, \tag{5}$$

where $\ominus$ is the erosion operator. Further, a recursive process is performed on J_1^n as $J_{k+1}^n = \max(J_k^n \ominus B_0, I)$ until no changes occur within a iteration which result in final grayscale reconstructed image J_∞^n for SE B_n.
In J_∞^n, the local minima smaller than B_n is filled in with a value proportional to the difference between max and min values within the neighborhood B_n. Therefore, the difference image $D = J_\infty^n - I$ infers potential airway locations and the algorithm is completed by combining maximum responses from different SEs.

2.3 Multi-Scale Vesselness Enhancement

Vessel enhancement algorithms are often employed to improve vascular structure identification and delineation. As shown in [4], analyzing the second-order information (Hessian) of a Gaussian convoluted image provides local information of the structure. Specifically, eigenvalue decomposition is performed over the Hessian matrix and the resulting ordered eigenvalues, i.e., $(|\lambda_1| \le |\lambda_2| \le |\lambda_3|)$, are examined. For voxels within vessels in particular, it is expected that λ_1 is small while the other two are large and of equal sign that indicates whether the vessel is brighter or darker than background. Explicitly, the vesselness can be formulated as

$$V_\sigma = \begin{cases} 0, & \text{if } \lambda_2 > 0 \text{ or } \lambda_3 > 0; \\ (1 - e^{-\frac{R_A^2}{2\alpha^2}}) e^{-\frac{R_B^2}{2\beta^2}} (1 - e^{-\frac{S^2}{2\gamma^2}}), & \text{otherwise,} \end{cases} \tag{6}$$

for a bright vessel on dark background, and $R_A = |\lambda_2|/|\lambda_3|$, $R_B = |\lambda_1|/|\lambda_2\lambda_3|$ and $S = \sqrt{\lambda_1^2 + \lambda_2^2 + \lambda_3^2}$. The vesselness measure above is calculated at different scales (σ) and the maximum response will be achieved at a scale that matches

the size of the vessel. Therefore, by using a multi-scale approach which covers a range of vessel widths and finding the maximum value $V = \max(V_\sigma), \sigma_{\min} \leq \sigma \leq \sigma_{\max}$, we get the vesselness measure as well as the approximate local vascular structure scale for each voxel in the image.

2.4 FC Based Multi-Scale Hybrid Region Growing

We developed a multi-scale hybrid region growing algorithm which adapts growing rules to local hanging-togetherness principle of FC method over image features given by intensity, grayscale morphological reconstruction, and vesselness enhancement. These features were used for the formulation of the fuzzy affinity function to facilitate RG.

Since effectiveness of FC is dependent on the choice of the affinity relation and a simple intensity based affinity relation may cause a leakage due to blurred and soft boundaries of the boundaries, enhancing airway structure and restoring continuity of the boundary is often desirable. For this purpose, vesselness filtering and grayscale morphological reconstruction can help identifying airway structures and provide continuity of the boundary, respectively. Note that the computation of grayscale morphological reconstruction is time consuming [2], and it yield non-significant contribution for segmentation of large airways. Therefore, it is efficient when only performed on small structures. Integrating features driven by vesselness filtering and grayscale morphological reconstruction processes into FC methodology is as follows.

The general setup for the affinity function can be divided to three components: adjacency μ_α, homogeneity μ_ψ and object feature μ_ϕ as

$$\mu_\kappa(p,q) = \begin{cases} 1, & \text{if } p = q; \\ \mu_\alpha(p,q)\sqrt{\mu_\psi(p,q)\mu_\phi(p,q)}, & \text{otherwise.} \end{cases} \quad (7)$$

Definition of the adjacency component is straightforward, $\mu_\alpha(p,q) = 1$, if p and q are adjacent to each other under 26-adjacency and '0' otherwise. $\mu_\psi(p,q)$ captures the homogeneity between p and q, with a smaller value for more similar pair. $\mu_\phi(p,q)$ also gives the hanging-togetherness of p and q in the target object based on likeliness of their feature values with respect to the expected feature distribution of the target object. For the algorithm discussed here, three features are available to describe for a given voxel x: intensity $I(x)$, grayscale morphological reconstructed result $D(x)$ and vesselness measurement $V(x)$ such that

$$F(x) = \{I(x), D(x), V(x)\}. \quad (8)$$

Moreover, the local scale information, $S(x)$, provided by multi-scale vesselness computation gives additional control over design of the affinity function since intensity is reliable for large airways while the other two features yield support for smaller ones.

The form of $\mu^f_\psi(p,q)$ and $\mu^f_\phi(p,q)$ with function $f(x)$ are

$$\mu^f_\psi(p,q) = e^{-\frac{|f(p)-f(q)|^2}{2\sigma^2_\psi}}, \quad (9)$$

$$\mu^f_\phi(p,q) = \min\left(e^{-\frac{|f(p)-m|^2}{2\sigma^2_\phi}}, e^{-\frac{|f(q)-m|^2}{2\sigma^2_\phi}}\right), \quad (10)$$

where σ_ψ and σ_ϕ are two different standard deviation parameters used for homogeneity and object feature distribution and m is the mean object feature value. For different features, we have $\mu^I_{\psi/\phi}$, $\mu^D_{\psi/\phi}$ and $\mu^V_{\psi/\phi}$ following the same formulation, and they are further combined as:

$$\mu^{FC}_{\psi/\phi} = \begin{cases} \mu^I_{\psi/\phi}, & \text{if } S > S_T; \\ k\mu^I_{\psi/\phi} + (1-k)\sqrt{\mu^D_{\psi/\phi}\mu^V_{\psi/\phi}}, & \text{otherwise,} \end{cases} \quad (11)$$

where S_T is the threshold for determining large airway where intensity is reliable and k is the factor to control the ratio of intensity as compared with the other two features in computing the final affinity function $\mu^{FC}_{\psi/\phi}$. It is expected that intensity plays a less important role for finer structures, so k may be formulated as $k = S/S_{\max}$ as $S_{\max}$ is the controlling parameter.

3 Results

In the context of segmentation, the "gold standard" is usually not available. Instead, manual delineation is often used as reference standard. However, for airway segmentation, especially in the presence of pulmonary diseases, this is extremely labor intensive since not only does it take many hours to segment a single lung CT scan, but it is also necessary to have a large and diverse dataset that covers images under various conditions. Here, we used the dataset and evaluation measurements provided by the EXACT'09 airway segmentation challenge [8]. Despite the fact that the training reference and the standard are not open to public and the extremely time consuming communication process makes only one-time evaluation possible, it is currently the best attempt towards validation for lung airway segmentation.

Fig. 2 shows the qualitative evaluation of our proposed method compared to two of the state-of-the-art methods. Here, we made our best effort to choose the same rendering scheme and 3-D viewing angles as the results provided by EXACT'09 for qualitative observation, although a minor miss alignment may still be unavoidable. For comparison purpose, we selected the best method in the sense of highest tree length detected rate under the restriction of low false positive rate (FPR) ($< 1\%$) which was produced by DIKU group who hosted the challenge. Also, the result given by UAVisionLab group was used as another reference since the quantitative difference between UAVisionLab and our method is comparable to the difference between our method and DIKU method. In the sense of algorithm complexity, UAVisionLab designed their method based on basic RG with a leakage control mechanism, while DIKU made use of vessel-airway relationship to formulate a more advanced voxel classification approach. The UAVisionLab method (a) detected tree length of 26.1% and FPR of 1.14%; DIKU group (b) detected tree length of 68.7% and FPR less than 0.01%; and our result (c) achieved detected tree length of 48.6% and FPR of 0.19%. From the statistics, we noticed that the difference in detected

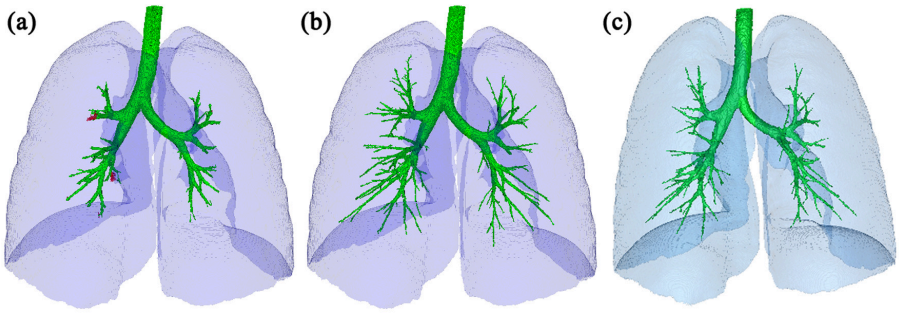

Fig. 2*:* 3-D Segmentation results on image CASE22 of EXACT'09 dataset [8]. (a) Result produced by UAVisionLab with detected tree length 26.1% and false positive rate 1.14%. (b)Result produced by DIKU with detected tree length 68.7% and false positive rate less than 0.01%. (c) Result produced by presented method with detected tree length 48.6% and false positive rate 0.19%. The red part in (a) shows the leakage.

tree length was about 20% with the difference between FPRs about 1 order of magnitude for both (a)-(c) and (b)-(c). However, as it visually appears, the difference between (b)-(c) is much more subtle than that of (a)-(c), which means the quantitative statistics is not actually "linearly related"to qualitative observation (and in the final result computation, we have left out an apparent outlier case). Since both (a) and (c) are based on RG, the improvement confirms the benefit provided by our proposed approach.

Table 1*:* Results of accuracy analysis of airway segmentation.

	Branch count	Branch detected (%)	Tree length (cm)	Leakage count
AVG	128.68	51.74	94.81	8.63
STD	58.68	10.55	43.51	10.45
	Tree length detected (%)	Leakage volume (mm^3)	False positive rate (FPR) (%)	
AVG	44.52	121.37	0.85	
STD	9.14	284.41	1.54	

The proposed method takes approximately 20 minutes for each test image. In the presented approach, the time for computationally involved grayscale morphological reconstruction is decreased by using a multi-scale approach. In addition, our method does not require any training process, which can be time consuming considering the need for a precise manual segmentation. The computational efficiency can be further improved by code optimization and multithreaded/parallel computation. Table 1 shows the statistics of the results, see [8] for details of each evaluation criteria as well as the statistics of other methods. Comparing with other state-of-the-art methods, the presented method achieves low average FPRs ($< 1\%$), hence it is comparable to those best methods, and *much more efficient* than the state-of-the-art methods in terms of computational burden (i.e. 20 vs 90 mins).

4 Conclusion

A new hybrid multi-scale airway segmentation algorithm has been developed. The proposed method combines vesselness and grayscale morphological reconstruction with FC facilitating region growth along thin airway structures. By incorporating multiple features to identify airway tree at different levels of scales, the algorithm adapts and governs the fuzzy segmentation process and captures airway under different pathological and imaging conditions more robustly in the presence of noise and other artifacts. The method is fully automatic with seed identification algorithm and the performance of the method has been qualitatively and quantitatively evaluated on human pulmonary CT images from diverse subjects. The results found are promising, which is shown to be superior in airway detection within methods with low false positive rates. Moreover, comparing with more advanced learning based methods, it takes much less time in producing segmentation results as well as human effort in generating manual training reference.

5 References

[1] M. Sonka, W. Park, and E. A. Hoffman, "Rule-based detection of intrathoracic airway trees," *IEEE Trans. Med. Imag.*, vol. 15, no. 3, pp. 314–326, 1996.

[2] D. Aykac, E. A. Hoffman, G. McLennan, and J. M. Reinhardt, "Segmentation and analysis of the human airway tree from three-dimensional X-ray CT images," *IEEE Trans. Med. Imag.*, vol. 22, no. 8, pp. 940–950, 2003.

[3] P. Lo, J. Sporring, H. Ashraf, J. J. H. Pedersen, and M. de Bruijne, "Vessel-guided airway tree segmentation: A voxel classification approach.," *Med. Imag. Ana.*, vol. 14, no. 4, pp. 527–538, 2010.

[4] A. Frangi, W. Niessen, K. Vincken, and M. Viergever, "Multiscale vessel enhancement filtering," in *MICCAI 1998*, 1998, vol. 1496, pp. 130–137.

[5] J. Pu, S. Gu, S. Liu, S. Zhu, D. Wilson, J. M. Siegfried, and D. Gur, "CT based computerized identification and analysis of human airways: A review," *Med. Phys.*, vol. 39, no. 5, pp. 2603–2616, 2012.

[6] J. K. Udupa and S. Samarasekera, "Fuzzy connectedness and object definition: Theory, algorithms, and applications in image segmentation," *CVGIP: Graph. Model & Imag. Proc.*, vol. 58, no. 3, pp. 246–261, 1996.

[7] M. Sonka, V. Hlavac, and R. Boyle, *Image Processing, Analysis, and Machine Vision*, Thomson-Engineering, 2007.

[8] P. Lo, B. van Ginneken, J. Reinhardt, and M. de Bruijne, "Extraction of airways from CT (EXACT'09)," in *Second International Workshop on Pulmonary Image Analysis*, 2009, pp. 175–189.